A residual a posteriori error estimate for the stabilization-free virtual element method

Journal of Computational Physics 553 (2026) 114704

Contents lists available at ScienceDirect

Journal of Computational Physics

journal homepage: www.elsevier.com/locate/jcp

A residual a posteriori error estimate for the stabilization-free virtual element method

Stefano Berrone, Andrea Borio, Davide Fassino *, Francesca Marcon

Dipartimento di Scienze Matematiche "Giuseppe Luigi Lagrange", Politecnico di Torino, Corso Duca degli Abruzzi 24, Torino, 10129, TO, Italy

A R T I C L E I N F O

2000 MSC:
65N15
65N22
65N30

Keywords:
Virtual element method
A posteriori error analysis
Stabilization-free

A B S T R A C T

In this work, we present the a posteriori error analysis of Stabilization-Free Virtual Element Methods for the 2D Poisson equation. The absence of a stabilizing bilinear form in the scheme allows to prove the equivalence between a suitably defined error measure and standard residual error estimators, which is not obtained in general for stabilized virtual elements. Several numerical experiments are carried out, confirming the expected behaviour of the estimator in the presence of different mesh types, and robustness with respect to jumps of the diffusion term.

1. Introduction

Virtual Element Methods (VEM) are a powerful technology enabling the solution to partial differential equations on general polytopal meshes. First introduced in Beirão da Veiga et al. [1], Beirão da Veiga et al. [2], this family of Galerkin methods is based on the definition of discrete spaces whose basis functions are not everywhere known analytically. Suitable discrete bilinear forms can be defined from the degrees of freedom, exploiting the computability of suitably defined polynomial projections of basis functions, which in general have a non-trivial kernel. Classical VEM bilinear forms also include a stabilizing operator, defined to take care of the kernel of the polynomial projections involved. Recently, the scientific community has invested a considerable effort in studying polynomial projection operators that are computable from the degrees of freedom of a VEM function and also stable. Starting from [3] and the preprint of [4], novel stabilization-free VEM have been devised for elliptic problems, based on polynomial projections of the gradients of basis functions on high degree polynomial spaces. In Berrone et al. [5,6], Borio et al. [7], Marcon and Mora [8], the theoretical foundations of the method were developed, considering the primal and mixed formulations of elliptic problems. Moreover, these discretization strategies have been applied to various problems of interest in computational mechanics [9–15].

This paper deals with the *a posteriori* error estimation of the scheme presented in [5,6]. In the context of classical stabilized VEM, the development of a posteriori error estimates can be found in [16–19] and adaptive schemes exploiting these results have been succesfully devised, addressing the non-trivial issue of defining quality-preserving refinement strategies for polygons [20]. However, in the a posteriori analysis of standard VEM the stabilization operator is found to be an issue in deriving the required equivalence between the error and the error estimator. Recently, some stabilization-free a posteriori error bounds were proved for stabilized VEM [21–23], though these results are limited to certain classes of meshes. In this work, the absence of a stabilizing bilinear form in stabilization-free schemes enables to prove rigorously the equivalence between a suitably defined error measure and classical

* Corresponding author.
E-mail addresses: stefano.berrone@polito.it (S. Berrone), andrea.borio@polito.it (A. Borio), davide.fassino@polito.it (D. Fassino), francesca.marcon@polito.it (F. Marcon).

https://doi.org/10.1016/j.jcp.2026.114704
Received 17 April 2025; Received in revised form 13 January 2026; Accepted 20 January 2026
Available online 29 January 2026

residual error estimators. A campaign of numerical tests confirms that the ratio between the error and the error estimator is indeed asymptotically constant. To streamline the analysis, estimates are presented in the case of a piecewise constant diffusivity coefficient $\mathcal{K}$. The extension to variable $\mathcal{K}$ would exploit analogous residual estimators and would yield a dependence of the estimate on local oscillations of the diffusivity coefficient, similarly to what happens in the *a posteriori* analysis of finite element methods.

The outline of the paper is as follows: in Sections 2 and 3 we introduce the model problem and describe the stabilization-free Virtual Element Method used to discretize the problem. In Section 4 we present the *a posteriori* error analysis of the numerical method. Section 5 is devoted to numerical results on a squared, an L-shaped domain, and on a Discrete Fracture Network, which models a fractured medium. Finally, in Section 6 we summarize the results and draw conclusions.

2. Model problem

Let $\Omega \subset \mathbb{R}^2$ be a bounded open set. We are interested in solving the following Poisson problem:

$$\begin{cases} -\nabla \cdot (\mathcal{K}\,\nabla u) = f & \text{in } \Omega, \\ u = 0 & \text{on } \partial\Omega, \end{cases} \tag{1}$$

where the loading term $f \in L^2(\Omega)$ and $\mathcal{K}$ is a symmetric tensor $\mathcal{K} \in (L^\infty(\Omega))^{2\times 2}$ satisfying:

$$\mathcal{K}_0|\boldsymbol{v}|^2 \le \boldsymbol{v}\cdot\mathcal{K}(\boldsymbol{x})\boldsymbol{v} \le \mathcal{K}_1|\boldsymbol{v}|^2, \quad \forall \boldsymbol{v}\in\mathbb{R}^2, \quad \text{for a.e. } \boldsymbol{x}\in\Omega, \tag{2}$$

where $\mathcal{K}_0$ and $\mathcal{K}_1$ are positive constants and $|\cdot|$ denotes the euclidean norm. We define the bilinear form $a(\cdot,\cdot):\ \mathrm{H}^1_0(\Omega)\times\mathrm{H}^1_0(\Omega)\to\mathbb{R}$ as

$$a(u,v) := \int_\Omega (\mathcal{K}\,\nabla u)\cdot\nabla v, \quad \forall\, u,v \in \mathrm{H}^1_0(\Omega). \tag{3}$$

The variational formulation of (1) reads as: find $u \in \mathrm{H}^1_0(\Omega)$ such that,

$$a(u,v) = (f,v)_\Omega \quad \forall\, v \in \mathrm{H}^1_0(\Omega), \tag{4}$$

where $(\cdot,\cdot)_{\mathcal{O}}$ denotes the scalar product in $L^2(\mathcal{O})$, where $\mathcal{O}\subseteq\Omega$.

3. Mesh and discretization

We introduce a conforming polygonal tessellation $\mathcal{M}_h$ of Ω. Let E denote a generic polygon of $\mathcal{M}_h$, h_E the diameter of E and the mesh size $h := \max_{E\in\mathcal{M}_h} h_E$. Furthermore, let $\mathcal{X}_h$ denote the set of vertices of $\mathcal{M}_h$. Moreover, let $\mathcal{E}_h$ be the set of edges of $\mathcal{M}_h$, $\mathcal{E}_h^{\text{int}}$ the set of edges of $\mathcal{M}_h$ internal to Ω and for each $E\in\mathcal{M}_h$ $\mathcal{E}_h^E := \{e\in\mathcal{E}_h : e\subset\partial E\}$. We assume that $\mathcal{M}_h$ satisfies the standard mesh assumptions for VEM, described below.

Assumption 3.1 (Mesh assumptions). $\exists\,\kappa>0$ such that $\forall E\in\mathcal{M}_h$,

- E is star-shaped with respect to a ball of radius $\rho_E \ge \kappa h_E$,
- for every edge $e\subset\partial E$, $|e| =: h_e \ge \kappa h_E$.

Notice that the above conditions imply that, denoting by N_E the number of vertices of E, the number of vertices of each polygon E has an upper bound, i.e.

$$\exists N_{\max} > 0 :\ \forall E\in\mathcal{M}_h,\ N_E \le N_{\max}\,. \tag{5}$$

Furthermore, these conditions ensure that the number of elements in the mesh sharing a vertex $\boldsymbol{x}\in\mathcal{X}_h$, denoted by $N^{\mathcal{X}}_{\boldsymbol{x}}$, remains bounded independently of h, i.e.

$$\exists N^{\mathcal{X}}_{\max} > 0 :\ \forall \boldsymbol{x}\in\mathcal{X}_h,\ N^{\mathcal{X}}_{\boldsymbol{x}} \le N^{\mathcal{X}}_{\max}\,. \tag{6}$$

From now on, for simplicity of exposition, we assume $\mathcal{K}$ to be a constant on each polygon $E\in\mathcal{M}_h$. Let $\mathcal{K}_E\in\mathbb{R}$ denote its value on each $E\in\mathcal{M}_h$.

3.1. Discretization

Let $\mathbb{P}_k(\mathcal{O})$ be the set of polynomials of degree up to k defined on an open connected set $\mathcal{O}$, and let $\mathbb{P}_m(\mathcal{O})\setminus\mathbb{P}_{n-1}(\mathcal{O})$ be the set of polynomials from degree n up to m. For any given $E\in\mathcal{M}_h$, let $\Pi_k^{\nabla,E} : \mathrm{H}^1(E)\to\mathbb{P}_k(E)$ be the H^1 orthogonal projection operator such that, $\forall\, u\in\mathrm{H}^1(E)$,

$$\begin{cases} \left(\nabla\left(\Pi_k^{\nabla,E}u - u\right),\nabla p\right)_E = 0 & \forall p\in\mathbb{P}_k(E) \\ \int_E u - \Pi_k^{\nabla,E}u = 0 & \text{if } k>1 \\ \int_{\partial E} u - \Pi_k^{\nabla,E}u = 0 & \text{if } k=1 \end{cases} \tag{7}$$

Moreover, we define the local Virtual Space of order k as

$$\mathcal{V}^E_{h,k} := \left\{v_h\in\mathrm{H}^1(E) : \Delta v_h\in\mathbb{P}_k(E),\ \gamma^e(v_h)\in\mathbb{P}_k(e)\ \forall e\subset\partial E, v_h\in C^0(\partial E),\ \left(v_h-\Pi_k^{\nabla,E}v_h, p\right)_E = 0\ \forall p\in\mathbb{P}_k(E)\setminus\mathbb{P}_{k-2}(E)\right\} \tag{8}$$

Given $v_h\in\mathcal{V}^E_{h,k}$, the chosen degrees of freedom of this space are:

- N_E pointwise values of v_h at the vertices of the polygon,
- if $k > 1$, $k-1$ pointwise values of v_h at Gauss-Lobatto quadrature points internal to each edge,
- if $k > 1$, $\frac{k(k-1)}{2}$ internal moments $\frac{1}{E}\left(v_h, m_i\right)_E$, $\forall\, i = 1, \dots, n_{k-2}$, where $n_{k-2} := \dim \mathbb{P}_{k-2}(E)$ and $\{m_i\}_{i=1}^{n_{k-2}}$ is a scaled monomial basis of $\mathbb{P}_{k-2}(E)$.

Then, we define the global discrete space as $\mathcal{V}_{h,k} := \{v \in \mathrm{H}^1_0(\Omega) : v_{|E} \in \mathcal{V}^E_{h,k}\}$.

To discretize (4), we follow the approach described in [6]. For any given $E \in \mathcal{M}_h$, let $\ell_E \geq 0$ be a given natural number and let $\mathcal{P}_{k,\ell_E}(E)$ be the polynomial space given by

$$\begin{aligned} \mathcal{P}_{k,\ell_E} &:= \left[\mathbb{P}_{k-1}(E)\right]^2 \oplus \mathbf{curl}\left(\mathbb{P}_{k+\ell_E}(E) \setminus \mathbb{P}_k(E)\right) \\ &= \boldsymbol{x}\mathbb{P}_{k-2}(E) \oplus \mathbf{curl}\,\mathbb{P}_{k+\ell_E}(E), \end{aligned} \tag{9}$$

where for any $p \in \mathbb{P}_{k+\ell_E}(E)$, $\mathbf{curl}\, p = \left(\frac{\partial p}{\partial x_2}, -\frac{\partial p}{\partial x_1}\right)$. Then, let $\Pi^{0,E}_{\mathcal{P}}\nabla : \mathrm{H}^1 + (E) \to \mathcal{P}_{k,\ell_E}$ be the L^2-projection operator of the gradient of functions in $\mathrm{H}^1(E)$, defined, $\forall u \in \mathrm{H}^1(E)$, by the orthogonality condition

$$\left(\Pi^{0,E}_{\mathcal{P}}\nabla u, \boldsymbol{p}\right)_E = (\nabla u, \boldsymbol{p})_E \quad \forall \boldsymbol{p} \in \mathcal{P}_{k,\ell_E}\,. \tag{10}$$

Remark 3.1. Notice that for each function $u_h \in \mathcal{V}^E_{h,k}$, the projection $\Pi^{0,E}_{\mathcal{P}}\nabla u_h$ is computable exploiting only the degrees of freedom of u_h.

Next, we define the discrete bilinear form $a^E_h : \mathcal{V}^E_{h,k} \times \mathcal{V}^E_{h,k} \to \mathbb{R}$ such that

$$a^E_h(u_h, v_h) := \left(\mathcal{K}_E \Pi^{0,E}_{\mathcal{P}}\nabla u_h, \Pi^{0,E}_{\mathcal{P}}\nabla v_h\right)_E, \quad \forall u_h, v_h \in \mathcal{V}^E_{h,k}\,, \tag{11}$$

Summing up over all the elements of $\mathcal{M}_h$, we define $a_h : \mathcal{V}_{h,k} \times \mathcal{V}_{h,k} \to \mathbb{R}$ as

$$a_h(u_h, v_h) := \sum_{E \in \mathcal{M}_h} a^E_h(u_h, v_h) \quad \forall u_h, v_h \in \mathcal{V}_{h,k}\,. \tag{12}$$

We can state the discrete problem as: find $u_h \in \mathcal{V}_{h,k}$ such that

$$a_h(u_h, v_h) = \sum_{E \in \mathcal{M}_h} \left(f_h, v_h\right)_E \quad \forall v_h \in \mathcal{V}_{h,k}\,, \tag{13}$$

where $f_h := \Pi^{0,E}_k f$ and $\forall E \in \mathcal{M}_h$, $\Pi^{0,E}_k : \mathrm{L}^2(E) \to \mathbb{P}_k(E)$ is the L^2-projection, defined $\forall u \in \mathrm{L}^2(E)$ by

$$\left(\Pi^{0,E}_k u, p\right)_E = (u, p)_E \quad \forall p \in \mathbb{P}_k(E)\,. \tag{14}$$

The well-posedness of (13) is discussed in [6]. We summarize it in the following result.

Assumption 3.2. We assume ℓ_E to be the smallest integer such that any polynomial $q \in \mathbb{P}_{k+\ell_E}(E)$ can be identified by a set of degrees of freedom which contains $kN_E - 1$ distinct moments $\frac{1}{|\partial E|}\left(q, \pi_i\right)_{\partial E}$ with respect to a scaled polynomial basis of the space $\mathbb{P}^0_{k-1}(\partial E) := \{\pi : \pi_{|_e} \in \mathbb{P}_{k-1}(e), \forall e \subset \partial E, \int_{\partial E} \pi = 0\}$.

Theorem 3.1. *Under the mesh Assumptions 3.1 and 3.2, there exists for any $E \in \mathcal{M}_h$ a constant α^E_* independent of h_E such that*

$$\left\|\Pi^{0,E}_{\mathcal{P}}\nabla v_h\right\|^2_{0,E} \geq \alpha^E_* \left\|\nabla v_h\right\|^2_{0,E}, \qquad \forall v_h \in \mathcal{V}_{h,E}.$$

Using the above result, it is immediate to see that (13) admits a unique solution under Assumption 3.2. In [6] it is also proved that Assumption 3.2 is also a necessary condition for well-posedness.

4. A posteriori error analysis

In this work, we consider as a measure of the error between the solution to problem (4) u and the solution to problem (13) u_h, the quantity

$$\begin{aligned} \left\|\!\left| u - u_h \right|\!\right\|_{\mathcal{K},1,\omega} &:= \sup_{w \in \mathrm{H}^1_0(\omega)} \frac{\sum_{E \in \omega} a^E(u, w) - a^E_h(u_h, w)}{\left\|\sqrt{\mathcal{K}}\nabla w\right\|_{0,\omega}} \\ &= \sup_{w \in \mathrm{H}^1_0(\omega)} \frac{\sum_{E \in \omega} \left(\mathcal{K}_E\left(\nabla u - \Pi^{0,E}_{\mathcal{P}}\nabla u_h\right), \nabla w\right)_E}{\left\|\sqrt{\mathcal{K}}\nabla w\right\|_{0,\omega}}, \end{aligned} \tag{15}$$

where $a|^E(\cdot,\cdot) := a(\cdot,\cdot)|_E$, and $\omega \subseteq \mathcal{M}_h$ is the union of the closure of a set of elements in $\mathcal{M}_h$.

Remark 4.1. We notice that if $u|_E \in \mathbb{P}_k(E)\ \forall E \in \mathcal{M}_h$, it results that
$\left\|\!\left| u - u_h \right|\!\right\|_{\mathcal{K},1,\omega} = 0$.

4.1. Preliminary results

In this section, we discuss some preliminary results that will be used in the definition of the upper and lower bounds of the error.

Lemma 4.1. *Let $E \in \mathcal{M}_h$, there exists a constant $C_p > 0$ independent of h_E, such that*

$$\left\| v - \Pi_k^{0,E} v \right\|_{0,E} \leq C_p \frac{h_E}{\sqrt{\mathcal{K}_E}} \left\| \sqrt{\mathcal{K}} \nabla v \right\|_{0,E}, \quad \forall v \in \mathrm{H}^1(E).$$

Proof. For any $E \in \mathcal{M}_h$, and function $v \in \mathrm{H}^1(E)$, we employ the Poincaré inequality, i.e.

$$\left\| v - \Pi_k^{0,E} v \right\|_{0,E} \leq \left\| v - \Pi_k^{0,E} v \right\|_{0,E} \leq C_p h_E \|\nabla v\|_{0,E} = C_p \frac{h_E}{\sqrt{\mathcal{K}_E}} \left\| \sqrt{\mathcal{K}} \nabla v \right\|_{0,E}.$$

□

In [17, Theorem 11] it has been proved the existence of the Clément quasi-interpolation operator for the VEM space, in order to give it, we recall some useful definitions.

Definition 4.1. For any element $E \in \mathcal{M}_h$, we define $\tilde{\omega}_E$ as the patch of elements with non-empty intersection with E, i.e. sharing at least one vertex. Furthermore, for any given $e \in \mathcal{E}_h$, let $\omega_e = \bigcup_{E \in \mathcal{M}_h : e \in \mathcal{E}_h^E} E$. Furthermore, $\tilde{\omega}_e = \bigcup_{E \in \omega_e} \tilde{\omega}_E$, and $\omega_E = \bigcup_{e \in \mathcal{E}_h^E} \omega_e$.

It can be proved that

$$N_{\max}^{\omega} = \max_{E \in \mathcal{M}_h} \{\#\tilde{\omega}_E\} \leq N_{\max}\left(N_{\max}^{\mathcal{X}} - 2\right) + 1, \tag{16}$$

where $N_{\max}$ and $N_{\max}^{\mathcal{X}}$ are defined in Assumption 3.1 and $\#\tilde{\omega}_E$ is the cardinality of $\tilde{\omega}_E$. Notice that, if $\mathcal{M}_h$ is a mesh of squares and E is an internal element, we get $\#\tilde{\omega}_E = 9$, achieving the equality in the above bound.

Lemma 4.2 (Clément interpolation estimates). *Under Assumption 3.1, for any $v \in \mathrm{H}_0^1(\Omega)$, there exists a Clément quasi-interpolation operator $v_I \in \mathcal{V}_{h,k}$ satisfying for each $E \in \mathcal{M}_h$*

$$\|v - v_I\|_{0,E} + h_E \|\nabla(v - v_I)\|_{0,E} \leq C_I h_E \|\nabla v\|_{0,\tilde{\omega}_E}, \tag{17}$$

where C_I is a positive constant, depending only on the polynomial degree k and on the mesh regularity.

Definition 4.2. For any given $e \in \mathcal{E}_h$, we define $\mathcal{K}_{\omega_e} = \sum_{E \in \omega_e} \mathcal{K}_E$.

Lemma 4.3. *Let v_I be the Clément quasi-interpolation operator as in Lemma 4.2, then there exist three positive constants $C_{I,1}$, $C_{\mathcal{K},E}$ and $C_{\mathcal{K}_{\omega_e}}$ such that, $\forall v \in \mathrm{H}_0^1(\Omega)$,*

$$\|v - v_I\|_{0,E} \leq C_I C_{\mathcal{K},E} \frac{h_E}{\sqrt{\mathcal{K}_E}} \left\| \sqrt{\mathcal{K}} \nabla v \right\|_{0,\tilde{\omega}_E} \qquad \forall E \in \mathcal{M}_h, \tag{18}$$

$$\|v - v_I\|_{0,e} \leq C_{I,1} C_{\mathcal{K}_{\omega_e}} \frac{h_e^{1/2}}{\sqrt{\mathcal{K}_{\omega_e}}} \left\| \sqrt{\mathcal{K}} \nabla v \right\|_{0,\tilde{\omega}_e} \qquad \forall e \in \mathcal{E}_h, \tag{19}$$

where $C_{\mathcal{K},E}, C_{\mathcal{K}_{\omega_e}}, C_{I,1}$ are positive constants, depending only on the polynomial degree k, on the mesh regularity and on the diffusivity coefficients $\mathcal{K}_E$. In particular, $C_{\mathcal{K},E} := \sqrt{\frac{\mathcal{K}_E}{\min_{E' \in \tilde{\omega}_E}\{\mathcal{K}_{E'}\}}}$, and $C_{\mathcal{K}_{\omega_e}} := \sum_{E \in \omega_e}\{C_{\mathcal{K},E}^2\}$.

Proof. Considering, (18), let $E \in \mathcal{M}_h$. From (17), we have that

$$\begin{aligned}
\|v - v_I\|_{0,E} &\leq C_I h_E \|\nabla v\|_{0,\tilde{\omega}_E} \leq C_I \frac{h_E}{\sqrt{\min_{E' \in \tilde{\omega}_E}\{\mathcal{K}_{E'}\}}} \left\| \sqrt{\mathcal{K}} \nabla v \right\|_{0,\tilde{\omega}_E} \\
&= C_I \frac{\sqrt{\mathcal{K}_E}}{\sqrt{\min_{E' \in \tilde{\omega}_E}\{\mathcal{K}_{E'}\}}} \frac{h_E}{\sqrt{\mathcal{K}_E}} \left\| \sqrt{\mathcal{K}} \nabla v \right\|_{0,\tilde{\omega}_E} = C_I C_{\mathcal{K},E} \frac{h_E}{\sqrt{\mathcal{K}_E}} \left\| \sqrt{\mathcal{K}} \nabla v \right\|_{0,\tilde{\omega}_E}.
\end{aligned}$$

Then, let $e \in \mathcal{E}_h$ be fixed. For any $E \in \omega_e$, we recall the following scaled trace inequality:

$$\|v\|_e^2 \leq C_{tr}\left(h_e^{-1}\|v\|_E^2 + h_e \|\nabla v\|_E^2\right), \quad \forall v \in H^1(E). \tag{20}$$

Then, by (20), (17), and Assumption 3.1, we have, $\forall E \in \omega_e$,

$$\begin{aligned}
\|v - v_I\|_{0,e}^2 &\leq C_{tr}\left(h_e^{-1}\|v - v_I\|_E^2 + h_e \|\nabla(v - v_I)\|_E^2\right) \\
&\leq C_{tr}\left(C_I^2 h_e^{-1} h_E^2 \|\nabla v\|_{0,\tilde{\omega}_E}^2 + C_I^2 h_e \|\nabla v\|_{0,\tilde{\omega}_E}^2\right) \\
&= C_{tr} C_I^2 \left(\frac{h_E^2}{h_e^2} + 1\right) h_e \|\nabla v\|_{0,\tilde{\omega}_E}^2
\end{aligned}$$

$$\leq C_{tr} C_I^2 \Big(\frac{1}{\kappa^2} + 1 \Big) C_{\mathcal{K},E}^2 \frac{h_e}{\mathcal{K}_E} \left\| \sqrt{\mathcal{K}} \nabla v \right\|_{0,\tilde{\omega}_E}^2 .$$

Hence,

$$\mathcal{K}_E \| v - v_I \|_{0,e}^2 \leq C_{tr} C_I^2 \Big(\frac{1}{\kappa^2} + 1 \Big) C_{\mathcal{K},E}^2 h_e \left\| \sqrt{\mathcal{K}} \nabla v \right\|_{0,\tilde{\omega}_E}^2 \quad \forall E \in \omega_e .$$

Summing up over $E \in \omega_e$, we obtain

$$\mathcal{K}_{\omega_e} \| v - v_I \|_{0,e}^2 \leq C_{I,1}^2 C_{\mathcal{K}_{\omega_e}}^2 h_e \left\| \sqrt{\mathcal{K}} \nabla v \right\|_{0,\tilde{\omega}_e}^2 .$$

where $C_{I,1}^2 := C_{tr} C_I^2 \Big(\frac{1}{\kappa^2} + 1 \Big)$. □

Lemma 4.4 (Galerkin orthogonality). *Let u be the solution to the continuous problem (4) and $u_h \in \mathcal{V}_{h,k}$ the solution to the discrete problem (13), it holds that*

$$a(u, w_h) - a_h(u_h, w_h) = \left(f - f_h, w_h \right)_\Omega \quad \forall w_h \in \mathcal{V}_{h,k} .$$

Proof. It follows immediately from the definition of the continuous problem(4) and the discrete problem (13). □

4.2. Upper bound of the error

Theorem 4.1 (Upper bound). *Let u be the solution to the continuous problem (4) and $u_h \in \mathcal{V}_{h,k}$ be the solution to the discrete problem (13). Then, there exists a constant $C_U > 0$ independent of h_E, depending on the mesh regularity, such that*

$$\| u - u_h \|_{\mathcal{K},1,\mathcal{M}_h}^2 \leq C_U \sum_{E \in \mathcal{M}_h} \left(\eta_E^2 + \mathcal{F}_E^2 \right), \tag{21}$$

where $\|\cdot\|_{\mathcal{K},1,\mathcal{M}_h}$ is defined by (15) and

$$\eta_E^2 := \frac{h_E^2}{\mathcal{K}_E} \| r_E \|_{0,E}^2 + \frac{1}{2} \sum_{e \in \mathcal{E}_h^E \cap \mathcal{E}_h^{\text{int}}} \frac{h_e}{\mathcal{K}_{\omega_e}} \| j_e \|_{0,e}^2 , \tag{22}$$

$$\mathcal{F}_E^2 := \frac{h_E^2}{\mathcal{K}_E} \| f - f_h \|_{0,E}^2 , \tag{23}$$

and

$$r_E := f_h + \div \Big(\mathcal{K}_E \, \Pi_{\mathcal{P}}^{0,E} \nabla u_h \Big), \tag{24}$$

$$j_e := [[\mathcal{K} \, \Pi_{\mathcal{P}}^0 \nabla u_h]]_e := \sum_{E \in \omega_e} \mathcal{K}_E \, \Pi_{\mathcal{P}}^{0,E} \nabla u_h \cdot \boldsymbol{n}_E^e , \tag{25}$$

where $\boldsymbol{n}_E^e$ is the normal vector to e pointing outward with respect to $E \in \omega_e$.

Proof. In the following, $\lesssim$ denotes the existence of a constant independent of h_E and $\mathcal{K}$. Let $w \in \mathrm{H}_0^1(\Omega)$ and $w_I \in \mathcal{V}_{h,k}$ such that it satisfies Lemma 4.2. By using Lemma 4.4 we have that

$$\begin{aligned} &\sum_{E \in \mathcal{M}_h} \Big(\mathcal{K}_E \Big(\nabla u - \Pi_{\mathcal{P}}^{0,E} \nabla u_h \Big), \nabla w \Big)_E = \\ &= \sum_{E \in \mathcal{M}_h} \Big(\mathcal{K}_E \Big(\nabla u - \Pi_{\mathcal{P}}^{0,E} \nabla u_h \Big), \nabla w - \nabla w_I \Big)_E + \left(f - f_h, w_I \right)_\Omega . \end{aligned}$$

Then, applying (4), it follows

$$\begin{aligned} &\sum_{E \in \mathcal{M}_h} \Big(\mathcal{K}_E \Big(\nabla u - \Pi_{\mathcal{P}}^{0,E} \nabla u_h \Big), \nabla w \Big)_E \\ &= \left(f, w - w_I \right)_\Omega - \sum_{E \in \mathcal{M}_h} \Big(\mathcal{K}_E \Pi_{\mathcal{P}}^{0,E} \nabla u_h, \nabla w - \nabla w_I \Big)_E + \left(f - f_h, w_I \right)_\Omega \\ &= \left(f - f_h, w - w_I \right)_\Omega + \left(f_h, w - w_I \right)_\Omega \\ &\qquad - \sum_{E \in \mathcal{M}_h} \Big(\mathcal{K}_E \Pi_{\mathcal{P}}^{0,E} \nabla u_h, \nabla w - \nabla w_I \Big)_E + \left(f - f_h, w_I \right)_\Omega \\ &= \left(f_h, w - w_I \right)_\Omega - \sum_{E \in \mathcal{M}_h} \Big(\mathcal{K}_E \Pi_{\mathcal{P}}^{0,E} \nabla u_h, \nabla w - \nabla w_I \Big)_E + \left(f - f_h, w \right)_\Omega . \end{aligned} \tag{26}$$

Considering the first two terms above, applying Green's theorem and since $w - w_I \in \mathrm{H}_0^1(\Omega)$, we have

$$\left(f_h, w - w_I \right)_\Omega - \sum_{E \in \mathcal{M}_h} \Big(\mathcal{K}_E \Pi_{\mathcal{P}}^{0,E} \nabla u_h, \nabla w - \nabla w_I \Big)_E$$

$$
\begin{aligned}
&= \sum_{E\in\mathcal{M}_h} \left(f_h + \div\left(\mathcal{K}_E\,\Pi^{0,E}_{\mathcal{P}}\nabla u_h\right), w - w_I\right)_E \\
&\quad - \sum_{e\in\mathcal{E}_h^{\mathrm{int}}} \left([[\mathcal{K}\,\Pi^{0,E}_{\mathcal{P}}\nabla u_h]]_e, w - w_I\right)_e \\
&= \sum_{E\in\mathcal{M}_h} \left(r_E, w - w_I\right)_E - \sum_{e\in\mathcal{E}_h^{\mathrm{int}}} \left(j_e, w - w_I\right)_e \\
&= I + II
\end{aligned}
$$

By employing (18) and with the definition $C_{\mathcal{K}} := \max_{E\in\mathcal{M}_h}\{C_{\mathcal{K},E}\}$, we get

$$
\begin{aligned}
I &= \sum_{E\in\mathcal{M}_h} \left(r_E, w - w_I\right)_E \le \sum_{E\in\mathcal{M}_h} \|r_E\|_{0,E}\|w - w_I\|_{0,E} \\
&\lesssim C_{\mathcal{K}} \sum_{E\in\mathcal{M}_h} \frac{h_E}{\sqrt{\mathcal{K}_E}}\|r_E\|_{0,E}\left\|\sqrt{\mathcal{K}}\nabla w\right\|_{0,\tilde{\omega}_E}.
\end{aligned}
$$

Using the Hölder inequality, we have

$$
I \lesssim C_{\mathcal{K}}\left(\sum_{E\in\mathcal{M}_h} \frac{h_E^2}{\mathcal{K}_E}\|r_E\|^2_{0,E}\right)^{1/2}\left(\sum_{E\in\mathcal{M}_h}\left\|\sqrt{\mathcal{K}}\nabla w\right\|^2_{0,\tilde{\omega}_E}\right)^{1/2}.
$$

On the other hand, employing (19) and the Hölder inequality, we obtain

$$
\begin{aligned}
II &= -\sum_{e\in\mathcal{E}_h^{\mathrm{int}}} \left(j_e, w - w_I\right)_e \le \sum_{e\in\mathcal{E}_h^{\mathrm{int}}} \|j_e\|_{0,e}\|w - w_I\|_{0,e} \\
&\lesssim C_{\mathcal{K}}^{\mathcal{E}_h^{\mathrm{int}}} \sum_{e\in\mathcal{E}_h^{\mathrm{int}}} \frac{h_e^{1/2}}{\sqrt{\mathcal{K}_{\omega_e}}}\|j_e\|_{0,e}\left\|\sqrt{\mathcal{K}}\nabla w\right\|_{0,\tilde{\omega}_e} \\
&\lesssim C_{\mathcal{K}}^{\mathcal{E}_h^{\mathrm{int}}}\left(\sum_{e\in\mathcal{E}_h^{\mathrm{int}}} \frac{h_e}{\mathcal{K}_{\omega_e}}\|j_e\|^2_{0,e}\right)^{1/2}\left(\sum_{e\in\mathcal{E}_h^{\mathrm{int}}}\left\|\sqrt{\mathcal{K}}\nabla w\right\|^2_{0,\tilde{\omega}_e}\right)^{1/2},
\end{aligned}
$$

where $C_{\mathcal{K}}^{\mathcal{E}_h^{\mathrm{int}}} := \max_{e\in\mathcal{E}_h^{\mathrm{int}}}\left\{C_{\mathcal{K}_{\omega_e}}\right\}$. We notice that from the mesh quality assumptions and the Definition 4.1 we have that

$$
\begin{aligned}
\left(\sum_{E\in\mathcal{M}_h}\left\|\sqrt{\mathcal{K}}\nabla w\right\|^2_{0,\tilde{\omega}_E}\right)^{1/2} &\le \sqrt{N^{\omega}_{\max}}\left\|\sqrt{\mathcal{K}}\nabla w\right\|_{0,\Omega}, \\
\left(\sum_{e\in\mathcal{E}_h^{\mathrm{int}}}\left\|\sqrt{\mathcal{K}}\nabla w\right\|^2_{0,\tilde{\omega}_e}\right)^{1/2} &\le \sqrt{2N^{\omega}_{\max}}\left\|\sqrt{\mathcal{K}}\nabla w\right\|_{0,\Omega},
\end{aligned}
$$

which bring the previous bounds to be

$$
I \lesssim C_{\mathcal{K}}\left(\sum_{E\in\mathcal{M}_h} \frac{h_E^2}{\mathcal{K}_E}\|r_E\|^2_{0,E}\right)^{1/2}\left\|\sqrt{\mathcal{K}}\nabla w\right\|_{0,\Omega}, \tag{27}
$$

$$
II \lesssim C_{\mathcal{K}}^{\mathcal{E}_h^{\mathrm{int}}}\left(\sum_{e\in\mathcal{E}_h^{\mathrm{int}}} \frac{h_e}{\mathcal{K}_{\omega_e}}\|j_e\|^2_{0,e}\right)^{1/2}\left\|\sqrt{\mathcal{K}}\nabla w\right\|_{0,\Omega}. \tag{28}
$$

Going back to (26), the last term can be estimated employing Lemma 4.1 and Hölder inequality, as follows:

$$
\begin{aligned}
\sum_{E\in\mathcal{M}_h}\left(f - f_h, w\right)_E &= \sum_{E\in\mathcal{M}_h}\left(f - f_h, w - \Pi^{0,E}_k w\right)_E \\
&\lesssim \sum_{E\in\mathcal{M}_h} \frac{h_E}{\sqrt{\mathcal{K}_E}}\|f - f_h\|_{0,E}\left\|\sqrt{\mathcal{K}}\nabla w\right\|_{0,E} \\
&\lesssim \left(\sum_{E\in\mathcal{M}_h} \frac{h_E^2}{\mathcal{K}_E}\|f - f_h\|^2_{0,E}\right)^{1/2}\left(\sum_{E\in\mathcal{M}_h}\left\|\sqrt{\mathcal{K}}\nabla w\right\|^2_{0,E}\right)^{1/2}.
\end{aligned}
$$

Summing up all the terms we get

$$
|||u - u_h|||_{\mathcal{K},1,\mathcal{M}_h} = \frac{\sum_{E\in\mathcal{M}_h}\left(\mathcal{K}_E\left(\nabla u - \Pi^{0,E}_{\mathcal{P}}\nabla u_h\right), \nabla w\right)_E}{\left\|\sqrt{\mathcal{K}}\nabla w\right\|_{0,\Omega}}
$$

$$\lesssim C_{\mathcal{K}}\left(\sum_{E\in\mathcal{M}_h}\frac{h_E^2}{\mathcal{K}_E}\|r_E\|_{0,E}^2\right)^{1/2}$$
$$+C_{\mathcal{K}}^{\mathcal{E}_h^{\mathrm{int}}}\left(\sum_{e\in\mathcal{E}_h^{\mathrm{int}}}\frac{h_e}{\mathcal{K}_{\omega_e}}\|j_e\|_{0,e}^2\right)^{1/2}+\left(\sum_{E\in\mathcal{M}_h}\frac{h_E^2}{\mathcal{K}_E}\|f-f_h\|_{0,E}^2\right)^{1/2}.$$

Then, the thesis is obtained as follows:

$$\begin{aligned}&|||u-u_h|||^2_{\mathcal{K},1,\mathcal{M}_h}\\ &\quad\lesssim C_U\sum_{E\in\mathcal{M}_h}\left(\frac{h_E^2}{\mathcal{K}_E}\|r_E\|_{0,E}^2+\sum_{e\in\mathcal{E}_h^E\cap\mathcal{E}_h^{\mathrm{int}}}\frac{h_e}{\mathcal{K}_{\omega_e}}\|j_e\|_{0,e}^2+\frac{h_E^2}{\mathcal{K}_E}\|f-f_h\|_{0,E}^2\right)\\ &\quad\lesssim C_U\sum_{E\in\mathcal{M}_h}\left(\eta_E^2+\mathcal{F}_E^2\right),\end{aligned}$$

where $C_U=\left(\max\{C_{\mathcal{K}},C_{\mathcal{K}}^{\mathcal{E}_h^{\mathrm{int}}},1\}\right)^2$. □

Remark 4.2. Following [24], assuming a quasi-monotonicity property on $\mathcal{K}$, it is possible to define a Clément-type quasi-interpolation operator satisfying error estimates that are independent of the local jumps of $\mathcal{K}$. In particular, in the proof of (18) we get

$$\|\nabla v\|_{0,\tilde{\omega}_E}\le\frac{1}{\sqrt{\mathcal{K}_E}}\left\|\sqrt{\mathcal{K}}\nabla v\right\|_{0,\tilde{\omega}_E},$$

and then $C_{\mathcal{K},E}=1$. Consequently in (19) we have $C_{\mathcal{K}_{\omega_e}}=1$ and in Theorem 4.1, the constant C_U does not depend on the diffusion $\mathcal{K}$.

4.3. Lower bound of the error

In order to prove the lower bound, we use the bubble function $\psi_E\in\mathrm{H}_0^1(E)$ for each $E\in\mathcal{M}_h$, as defined in [16,17]. In particular, we build a shape-regular sub-triangulation of E and define ψ_E as the sum of the barycentric bubble functions, which are polynomials on each sub-triangle. As done in [25], for any element $E\in\mathcal{M}_h$, we define the function

$$w_{r,E}(x):=\begin{cases}\frac{h_E^2}{\mathcal{K}_E}r_E(x)\psi_E(x) & x\in E\,,\\ 0 & x\in\Omega\setminus E\,,\end{cases}\tag{29}$$

where r_E is defined by (24). Since r_E is a polynomial, using the techniques in [25,26], the following results hold true.

Lemma 4.5. *Let $E\in\mathcal{M}_h$ and $w_{r,E}$ the corresponding function defined above. The following inequalities hold true*

$$\frac{h_E^2}{\mathcal{K}_E}\|r_E\|_{0,E}^2\le C_{1,B}\left(r_E,w_{r,E}\right)_E,$$

and

$$h_E\|\nabla w_{r,E}\|_{0,E}\le C_{2,B}\frac{h_E^2}{\mathcal{K}_E}\|r_E\|_{0,E},$$

where $C_{1,B}$, $C_{2,B}$ are constants independent of h_E and $\mathcal{K}$,but depending on the mesh regularity.

Remark 4.3. From the definition of the space (9), it is immediate to check that $\div\Pi_p^{0,E}\nabla u\in\mathbb{P}_{k-2}(E)$. Thus, since $f_h\in\mathbb{P}_k(E)$, $r_E\in\mathbb{P}_k(E)$, which implies that the constants $C_{1,B}$ and $C_{2,B}$ in Lemma 4.5 do not depend on ℓ_E.

Similarly, for any given $e\in\mathcal{E}_h^{\mathrm{int}}$, let ψ_e be the bubble function relative to e, as defined in [16,17]. In particular, we consider the sub-triangles sharing e of the elements in ω_e and ψ_e is defined as the sum of the barycentric bubble functions relative to these sub-triangles. Moreover, following [26] we extend j_e, defined by (25), through a constant prolongation in the normal direction with respect to e. Let Cj_e be such function. We define

$$w_{j,e}(x):=\begin{cases}\frac{h_e}{\mathcal{K}_{\omega_e}}(Cj_e)(x)\psi_e(x) & x\in\omega_e,\\ 0 & x\in\Omega\setminus\omega_e\,.\end{cases}\tag{30}$$

The following results can be proved using the techniques in [25,26].

Lemma 4.6. *Let $E\in\mathcal{M}_h$, $e\in\mathcal{E}_h^E$ and $w_{j,E}$ as defined in (30). Then,*

$$\frac{h_e}{\mathcal{K}_{\omega_e}}\|j_e\|_{0,e}^2\le C_{1,b}\left(j_e,w_{j,e}\right)_e,$$

and

$$h_e^{1/2}\left\|\nabla w_{j,e}\right\|_{0,E} \leq C_{2,b}\frac{h_e}{\mathcal{K}_{\omega_e}}\|j_e\|_{0,e},$$

where $C_{1,b}$, $C_{2,b}$ are constants independent of h_E and $\mathcal{K}$, but depending on the mesh regularity.

Theorem 4.2 (Local lower bound)**.**

Let $E \in \mathcal{M}_h$ be given, u the solution to the continuous problem (4) and $u_h \in \mathcal{V}_{h,k}$ the solution to the discrete problem (13). Then there exists a constant $C_L > 0$ independent of h_E and of $\mathcal{K}$, but depending on the mesh regularity, such that

$$\eta_E^2 \leq C_L\left(\left\|\left|u-u_h\right|\right\|^2_{\mathcal{K},1,\omega_E} + \sum_{E\in\omega_E}\mathcal{F}_E^2\right),$$

where $\left\|\left|u-u_h\right|\right\|_{\mathcal{K},1,\omega_E}$ is defined by (15) and η_E and $\mathcal{F}_E$ in Theorem 4.1.

Proof. In the following, $\lesssim$ denotes the existence of a constant independent of h_E and $\mathcal{K}$. For any $w \in \mathrm{H}^1_0(\Omega)$, exploiting problems (4) and (13) and the definitions of r_E and j_e in (24)-(25), we have

$$\begin{aligned}
&\sum_{E\in\mathcal{M}_h}\left(\mathcal{K}_E\left(\nabla u - \Pi^{0,E}_{\mathcal{P}}\nabla u_h\right),\nabla w\right)_E = \\
&= \sum_{E\in\mathcal{M}_h}(f,w)_E - \sum_{E\in\mathcal{M}_h}\left(\mathcal{K}_E\Pi^{0,E}_{\mathcal{P}}\nabla u_h,\nabla w\right)_E \\
&= \sum_{E\in\mathcal{M}_h}(f_h,w)_E - \sum_{E\in\mathcal{M}_h}\left(\mathcal{K}_E\Pi^{0,E}_{\mathcal{P}}\nabla u_h,\nabla w\right)_E + \sum_{E\in\mathcal{M}_h}(f-f_h,w)_E \\
&= \sum_{E\in\mathcal{M}_h}(f_h,w)_E + \sum_{E\in\mathcal{M}_h}\left(\div\left(\mathcal{K}_E\Pi^{0,E}_{\mathcal{P}}\nabla u_h\right),w\right)_E \\
&\quad - \sum_{e\in\mathcal{E}_h^{\text{int}}}\left([[\mathcal{K}\,\Pi^0_{\mathcal{P}}\nabla u_h]]_e,w\right)_e + \sum_{E\in\mathcal{M}_h}(f-f_h,w)_E \\
&= \sum_{E\in\mathcal{M}_h}(r_E,w)_E - \sum_{e\in\mathcal{E}_h^{\text{int}}}(j_e,w)_e + \sum_{E\in\mathcal{M}_h}(f-f_h,w)_E\,.
\end{aligned} \tag{31}$$

First, taking $w = w_{r,E}$ as defined in (29), since $\operatorname{supp}(w_{r,E}) \subseteq E$ we get

$$\left(\mathcal{K}_E\left(\nabla u - \Pi^{0,E}_{\mathcal{P}}\nabla u_h\right),\nabla w_{r,E}\right)_E = \left(f-f_h,w_{r,E}\right)_E + \left(r_E,w_{r,E}\right)_E.$$

Using the Cauchy-Schwarz inequality and Lemma 4.5, we have that

$$\begin{aligned}
\frac{h_E^2}{\mathcal{K}_E}\|r_E\|^2_{0,E} &\lesssim \left(\mathcal{K}_E\left(\nabla u - \Pi^{0,E}_{\mathcal{P}}\nabla u_h\right),\nabla w_{r,E}\right)_E + \left(f_h-f,w_{r,E}\right)_E \\
&\lesssim \left(\mathcal{K}_E\left(\nabla u - \Pi^{0,E}_{\mathcal{P}}\nabla u_h\right),\nabla w_{r,E}\right)_E + \|f-f_h\|_{0,E}\|w_{r,E}\|_{0,E} \\
&\lesssim \left(\mathcal{K}_E\left(\nabla u - \Pi^{0,E}_{\mathcal{P}}\nabla u_h\right),\nabla w_{r,E}\right)_E \\
&\quad + \left(\frac{h_E^2}{\mathcal{K}_E}\|f-f_h\|^2_{0,E}\right)^{1/2}\left\|\sqrt{\mathcal{K}}\nabla w_{r,E}\right\|_{0,E}.
\end{aligned}$$

Then,

$$\frac{\frac{h_E^2}{\mathcal{K}_E}\|r_E\|^2_{0,E}}{\left\|\sqrt{\mathcal{K}}\nabla w_{r,E}\right\|_{0,E}} \lesssim \left\|\left|u-u_h\right|\right\|_{\mathcal{K},1,E} + \left(\frac{h_E^2}{\mathcal{K}_E}\|f-f_h\|^2_{0,E}\right)^{1/2}. \tag{32}$$

We notice that, from Lemma 4.5, one has

$$\left\|\sqrt{\mathcal{K}}\nabla w_{r,E}\right\|_{0,E} = \sqrt{\mathcal{K}_E}\|\nabla w_{r,E}\|_{0,E} \lesssim \frac{h_E}{\sqrt{\mathcal{K}_E}}\|r_E\|_{0,E}.$$

Then, from (32) we get

$$\frac{h_E}{\sqrt{\mathcal{K}_E}}\|r_E\|_{0,E} \lesssim \left\|\left|u-u_h\right|\right\|_{\mathcal{K},1,E} + \left(\frac{h_E^2}{\mathcal{K}_E}\|f-f_h\|^2_{0,E}\right)^{1/2},$$

and, squaring,

$$\frac{h_E^2}{\mathcal{K}_E}\|r_E\|^2_{0,E} \lesssim \left(\left\|\left|u-u_h\right|\right\|^2_{\mathcal{K},1,E} + \frac{h_E^2}{\mathcal{K}_E}\|f-f_h\|^2_{0,E}\right). \tag{33}$$

Going back to (31), for any edge $e \in \mathcal{E}_h^{\text{int}}$ we take $w = w_{j,e}$ as defined in (30). Since $\text{supp}(w_{j,e}) \subseteq \omega_e$ we get

$$\sum_{E \in \omega_e} \left(\mathcal{K}_E \left(\nabla u - \Pi_{\mathcal{P}}^{0,E} \nabla u_h \right), \nabla w_{j,e} \right)_E = \sum_{E \in \omega_e} \left(r_E, w_{j,e} \right)_E - \left(j_e, w_{j,e} \right)_e + \sum_{E \in \omega_e} \left(f - f_h, w_{j,e} \right)_E .$$

Using Lemma 4.6 and the Hölder and Poincaré inequalities, we get

$$\begin{aligned} \frac{h_e}{\mathcal{K}_{\omega_e}} \| j_e \|_{0,e}^2 &\lesssim \sum_{E \in \omega_e} \left(\left(r_E, w_{j,e} \right)_E + \left(f - f_h, w_{j,e} \right)_E \right) - \sum_{E \in \omega_e} \left(\mathcal{K}_E \left(\nabla u - \Pi_{\mathcal{P}}^{0,E} \nabla u_h \right), \nabla w_{j,e} \right)_E \\ &\lesssim \sum_{E \in \omega_e} \frac{h_E}{\sqrt{\mathcal{K}_E}} \| r_E \|_{0,E} \left\| \sqrt{\mathcal{K}} \nabla w_{j,e} \right\|_{0,E} + \sum_{E \in \omega_e} \frac{h_E}{\sqrt{\mathcal{K}_E}} \| f - f_h \|_{0,E} \left\| \sqrt{\mathcal{K}} \nabla w_{j,e} \right\|_{0,E} \\ &\quad - \sum_{E \in \omega_e} \left(\mathcal{K}_E \left(\nabla u - \Pi_{\mathcal{P}}^{0,E} \nabla u_h \right), \nabla w_{j,e} \right)_E \\ &\lesssim \left(\sum_{E \in \omega_e} \frac{h_E^2}{\mathcal{K}_E} \| r_E \|_{0,E}^2 \right)^{1/2} \left(\sum_{E \in \omega_e} \left\| \sqrt{\mathcal{K}} \nabla w_{j,e} \right\|_{0,E}^2 \right)^{1/2} \\ &\quad + \left(\sum_{E \in \omega_e} \frac{h_E^2}{\mathcal{K}_E} \| f - f_h \|_{0,E}^2 \right)^{1/2} \left(\sum_{E \in \omega_e} \left\| \sqrt{\mathcal{K}} \nabla w_{j,e} \right\|_{0,E}^2 \right)^{1/2} \\ &\quad - \sum_{E \in \omega_e} \left(\mathcal{K}_E \left(\nabla u - \Pi_{\mathcal{P}}^{0,E} \nabla u_h \right), \nabla w_{j,e} \right)_E . \end{aligned}$$

Then, employing the definition of $|||u - u_h|||_{\mathcal{K},1,\omega_e}$ in (15),

$$\begin{aligned} &\frac{\frac{h_e}{\mathcal{K}_{\omega_e}} \| j_e \|_{0,e}^2}{\left(\sum_{E \in \omega_e} \left\| \sqrt{\mathcal{K}} \nabla w_{j,e} \right\|_{0,E}^2 \right)^{1/2}} \\ &\lesssim \left(\sum_{E \in \omega_e} \frac{h_E^2}{\mathcal{K}_E} \| r_E \|_{0,E}^2 \right)^{1/2} + \left(\sum_{E \in \omega_e} \frac{h_E^2}{\mathcal{K}_E} \| f - f_h \|_{0,E}^2 \right)^{1/2} \\ &\quad + \frac{\sum_{E \in \omega_e} \left(\mathcal{K}_E \left(\nabla u - \Pi_{\mathcal{P}}^{0,E} \nabla u_h \right), \nabla (-w_{j,e}) \right)_E}{\left(\sum_{E \in \omega_e} \left\| \sqrt{\mathcal{K}} \nabla (-w_{j,e}) \right\|_{0,E}^2 \right)^{1/2}} \\ &\lesssim \left(\sum_{E \in \omega_e} \frac{h_E^2}{\mathcal{K}_E} \| r_E \|_{0,E}^2 \right)^{1/2} + \left(\sum_{E \in \omega_e} \frac{h_E^2}{\mathcal{K}_E} \| f - f_h \|_{0,E}^2 \right)^{1/2} + |||u - u_h|||_{\mathcal{K},1,\omega_e} . \end{aligned} \tag{34}$$

We employ again Lemma 4.6, obtaining

$$\left(\sum_{E \in \omega_e} \left\| \sqrt{\mathcal{K}} \nabla w_{j,e} \right\|_{0,E}^2 \right)^{1/2} \lesssim \left(\sum_{E \in \omega_e} \mathcal{K}_E \frac{h_e}{\mathcal{K}_{\omega_e}^2} \| j_e \|_{0,e}^2 \right)^{1/2} + \left(\frac{h_e}{\mathcal{K}_{\omega_e}} \| j_e \|_{0,e}^2 \right)^{1/2} .$$

Thus, subtituting in (34), we get

$$\begin{aligned} \left(\frac{h_e}{\mathcal{K}_{\omega_e}} \| j_e \|_{0,e}^2 \right)^{1/2} &\lesssim \left(\sum_{E \in \omega_e} \frac{h_E^2}{\mathcal{K}_E} \| r_E \|_{0,E}^2 \right)^{1/2} \\ &\quad + \left(\sum_{E \in \omega_e} \frac{h_E^2}{\mathcal{K}_E} \| f - f_h \|_{0,E}^2 \right)^{1/2} + |||u - u_h|||_{\mathcal{K},1,\omega_e} . \end{aligned}$$

and squaring,

$$\frac{h_e}{\mathcal{K}_{\omega_e}} \| j_e \|_{0,e}^2 \lesssim \sum_{E \in \omega_e} \frac{h_E^2}{\mathcal{K}_E} \| r_E \|_{0,E}^2 + \sum_{E \in \omega_e} \frac{h_E^2}{\mathcal{K}_E} \| f - f_h \|_{0,E}^2 + |||u - u_h|||_{\mathcal{K},1,\omega_e}^2 . \tag{35}$$

Finally, we apply (33) in (35), getting

$$\frac{h_e}{\mathcal{K}_{\omega_e}} \| j_e \|_{0,e}^2 \lesssim \sum_{E \in \omega_e} \frac{h_E^2}{\mathcal{K}_E} \| f - f_h \|_{0,E}^2 + |||u - u_h|||_{\mathcal{K},1,\omega_e}^2 . \tag{36}$$

We conclude the proof by summing (33) and (36). □

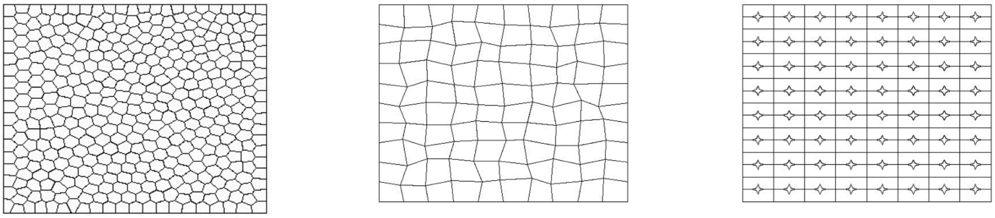

(a) `Polymesher` (b) `Distorted cartesian` (c) `Star concave`

Fig. 1. Meshes used for convergence tests.

Corollary 4.1 (Global lower bound). *Let u the solution to the continuous problem (4) and $u_h \in \mathcal{V}_{h,k}$ the solution to the discrete problem (13).*
Let $\|\|u - u_h\|\|_{\mathcal{K},1,\mathcal{M}_h}$ be defined as in (15), it holds

$$\sum_{E\in\mathcal{M}_h} \eta_E^2 \leq C_L(N_{\max}+1)\left(\|\|u-u_h\|\|^2_{\mathcal{K},1,\mathcal{M}_h} + \sum_{E\in\mathcal{M}_h} \mathcal{F}_E^2 \right),$$

where η_E, $\mathcal{F}_E$ are defined in Theorem 4.1, C_L is defined in Theorem 4.2, and $N_{\max}$ as in Assumption 3.1.

5. Numerical results

In this section, we present some numerical tests to show the equivalence between error and error estimator in the different problems proposed in [16] and on a standard test on an L-shaped domain. Firstly, we approximate the error defined in (15) as

$$\|\|u-u_h\|\|_{\mathcal{K},1,\mathcal{M}_h} \simeq \left(\sum_{E\in\mathcal{M}_h} \left\| \sqrt{\mathcal{K}}\left(\nabla u - \Pi_{\mathcal{P}}^{0,E}\nabla u_h\right)\right\|^2_{0,E}\right)^{\frac{1}{2}},$$

and define the *effectivity index* as the ratio between the estimator and the error, i.e.

$$\epsilon := \left(\frac{\sum_{E\in\mathcal{M}_h} \eta_E^2}{\sum_{E\in\mathcal{M}_h} \left\| \sqrt{\mathcal{K}}\left(\nabla u - \Pi_{\mathcal{P}}^{0,E}\nabla u_h\right)\right\|^2_{0,E}} \right)^{\frac{1}{2}}.$$

5.1. Test 1

We consider the Poisson problem with $\mathcal{K} = I$ and $\Omega = (0,1)^2$, setting the loading term f in such a way that the solution to the problem is $u(x,y) = \sin(2\pi x)\sin(2\pi y)$. We tested it on meshes made up of convex polygons labeled `Polymesher` [27], distorted cartesian meshes (`Distorted cartesian`), and concave meshes labeled `Star concave`, as represented in Fig. 1. Fig. 2 shows the behavior of the estimator and the errors in the cases $k = 1,2,3$. Moreover, they show that the effectivity indices are independent of the meshsize and display a weak dependence on the type of polygons used.

5.2. Test 2

We test the estimator in the presence of diffusion jumps. Let $\Omega = (0,1)^2$ and the diffusion tensor $\mathcal{K}(x,y) = \gamma_i(x,y)I$, $i = 1,2$, and

$$\gamma_1(x,y) := \begin{cases} 10, \text{ in } \Omega_1 := (0,0.5]\times(0,1), \\ 1, \text{ in } \Omega_2 := (0.5,1)\times(0,1), \end{cases} \quad \gamma_2(x,y) := \begin{cases} 10^{-3}, \text{ in } \Omega_1, \\ 1, \text{ in } \Omega_2. \end{cases}$$

The loading term is chosen so that the solution $u_i(x,y) = \xi_i(x)Y(y)$, where

$$\xi_i(x) := \begin{cases} -\frac{1}{\gamma_i|_{\Omega_1}}\left(\frac{x^2}{2} + c_i x\right) & \text{if } x \in (0,0.5], \\ -\frac{1}{\gamma_i|_{\Omega_2}}\left(\frac{x^2}{2} + c_i x - c_i - \frac{1}{2}\right) & \text{if } x \in (0.5,1), \end{cases} \tag{37}$$

$$Y(y) := y(1-y)\left(y - \frac{1}{2}\right)^2, \tag{38}$$

and $c_i := -\frac{3\gamma_i|_{\Omega_1} + \gamma_i|_{\Omega_2}}{4\left(\gamma_i|_{\Omega_1} + \gamma_i|_{\Omega_2}\right)}$.

We solve the problem on a family of distorted cartesian meshes (see Fig. 1b), conforming to the jumps of $\mathcal{K}$. The convergence plots displayed in Fig. 3 confirm the optimal convergence rates. The effectivity indices remain stable with respect to the meshsize. The jump of the diffusivity coefficient has a minimal impact on the indices ϵ, demonstrating strong robustness of the estimator.

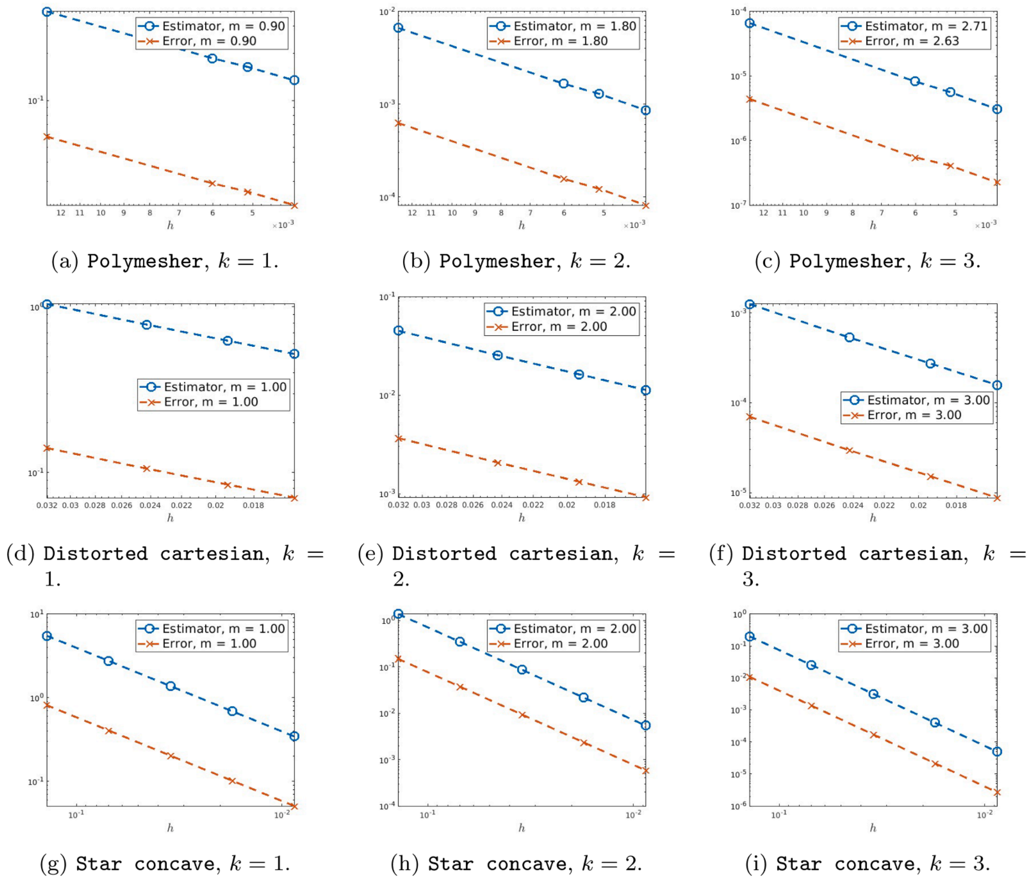

(a) `Polymesher`, $k = 1$. (b) `Polymesher`, $k = 2$. (c) `Polymesher`, $k = 3$.

(d) `Distorted cartesian`, $k = 1$. (e) `Distorted cartesian`, $k = 2$. (f) `Distorted cartesian`, $k = 3$.

(g) `Star concave`, $k = 1$. (h) `Star concave`, $k = 2$. (i) `Star concave`, $k = 3$.

Fig. 2. Test 1: Convergence plots. In the legends, *m* is the average convergence rate.

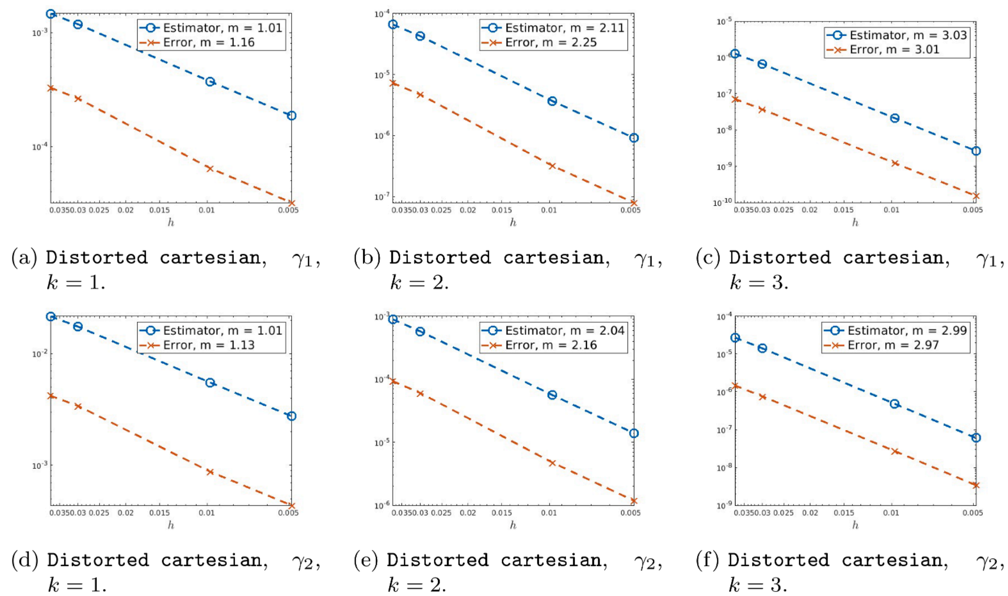

(a) `Distorted cartesian`, γ_1, $k = 1$. (b) `Distorted cartesian`, γ_1, $k = 2$. (c) `Distorted cartesian`, γ_1, $k = 3$.

(d) `Distorted cartesian`, γ_2, $k = 1$. (e) `Distorted cartesian`, γ_2, $k = 2$. (f) `Distorted cartesian`, γ_2, $k = 3$.

Fig. 3. Test 2: Convergence plots. In the legends, *m* is the average convergence rate.

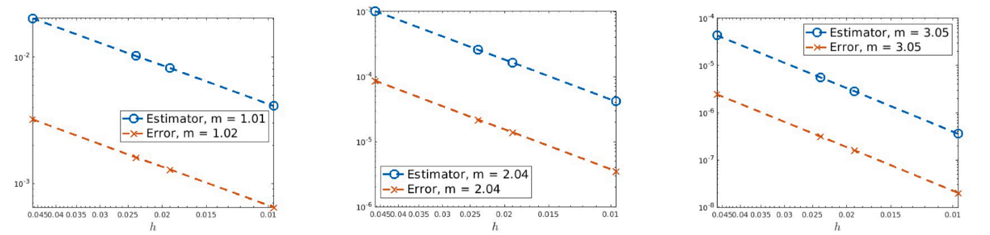

(a) `Distorted cartesian`, γ_3, $k = 1$. (b) `Distorted cartesian`, γ_3, $k = 2$. (c) `Distorted cartesian`, γ_3, $k = 3$.

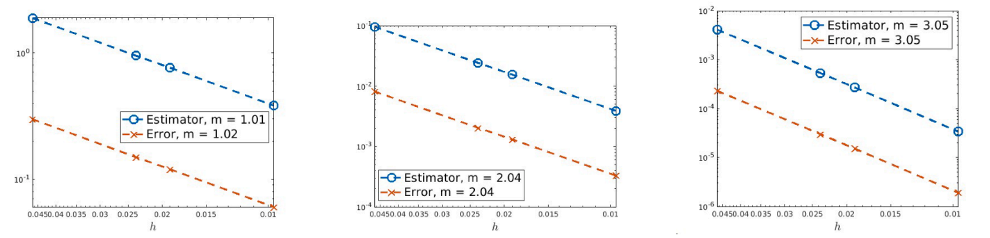

(d) `Distorted cartesian`, γ_4, $k = 1$. (e) `Distorted cartesian`, γ_4, $k = 2$. (f) `Distorted cartesian`, γ_4, $k = 3$.

Fig. 4. Test 3: Convergence plots. In the legends, m is the average convergence rate.

5.3. Test 3

In this section, we consider problems where the diffusity coefficient does not meet the quasi-monotonicity condition discussed in Remark 4.2. The tests considered are the one presented in [24], where $\Omega = (0,1)^2$ and the diffusion tensor is $\mathcal{K} = \gamma_i I$ with $i = 3, 4$, with

$$\gamma_3(x,y) := \begin{cases} 1 \quad \text{in } \Omega_{11} = (0, 0.5)^2, \\ 10^{-3} \quad \text{in } \Omega_{12} = [0.5, 1) \times (0, 0.5), \\ 10^{-2} \quad \text{in } \Omega_{21} = (0, 0.5) \times [0.5, 1), \\ 10 \quad \text{in } \Omega_{22} = [0.5, 1)^2, \end{cases} \qquad \gamma_4(x,y) := \begin{cases} 1 \quad \text{in } \Omega_{11}, \\ 10^{-7} \quad \text{in } \Omega_{12}, \\ 10^{-2} \quad \text{in } \Omega_{21}, \\ 10^{5} \quad \text{in } \Omega_{22}, \end{cases}$$

We impose the loading terms in such a way that the exact solutions are

$$u_i(x,y) = \xi_i(x) Y(y),$$

where $\xi_i(x)$, $Y(y)$ are defined in (37) and in (38), and

$$c_i := \begin{cases} -\dfrac{3\gamma_i|_{\Omega_{11}} + \gamma_i|_{\Omega_{12}}}{4\left(\gamma_i|_{\Omega_{11}} + \gamma_i|_{\Omega_{12}}\right)} & \text{in } \Omega_{11} \cup \Omega_{12}, \\ -\dfrac{3\gamma_i|_{\Omega_{21}} + \gamma_i|_{\Omega_{22}}}{4\left(\gamma_i|_{\Omega_{21}} + \gamma_i|_{\Omega_{22}}\right)} & \text{in } \Omega_{21} \cup \Omega_{22}. \end{cases}$$

We solve the problem on a family of distorted cartesian meshes (see Fig. 1b), conforming to the jumps of $\mathcal{K}$, achieving the optimal convergence rate as shown in Fig. 4. The results show that the computed effectivity indices are independent of the meshsize, proving the robustness of the estimate proposed. We notice also in this case that the jumps of $\mathcal{K}$ do not influence significantly the effectivity indices, even though the quasi-monotonicity property is not fulfilled. Indeed, the area of the polygons where the quasi-monotonicity of $\mathcal{K}$ is not satisfied is decreasing with h.

5.4. Test 4

We consider a problem defined on the L-shaped domain $\Omega = (-1,1)^2 \setminus ([0,1] \times [-1,0])$. We take the boundary conditions and the loading term such that the solution results

$$u(\rho, \theta) = \rho^{2/3},$$

where ρ and θ are the polar coordinates. This solution $u \in \mathrm{H}^1(\Omega)$ has a corner singularity in the origin, and it is possible to prove that $u \in \mathrm{H}^s(\Omega)$, $s < \frac{5}{3}$. Under uniform mesh refinements, the asymptotic rate is suboptimal and it results $\left(\#\mathcal{M}_h\right)^{-1/3} \simeq h^{2/3}$, independently on the polynomial degree k. We performed the test on `Polymesher`, `Distorted cartesian`, and `Star concave` L-shaped meshes (see Fig. 5) and for the cases $k = 1, 2, 3$, achieving the expected order of convergence as shown in Fig. 6. The test highlights that the effectivity indices are not affected by the bounded Sobolev regularity of the problem.

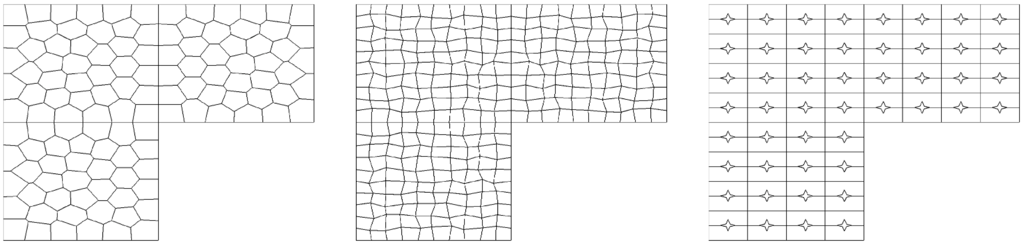

(a) `Polymesher` (b) `Distorted cartesian` (c) `Star concave`

Fig. 5. Meshes used for convergence Test 4.

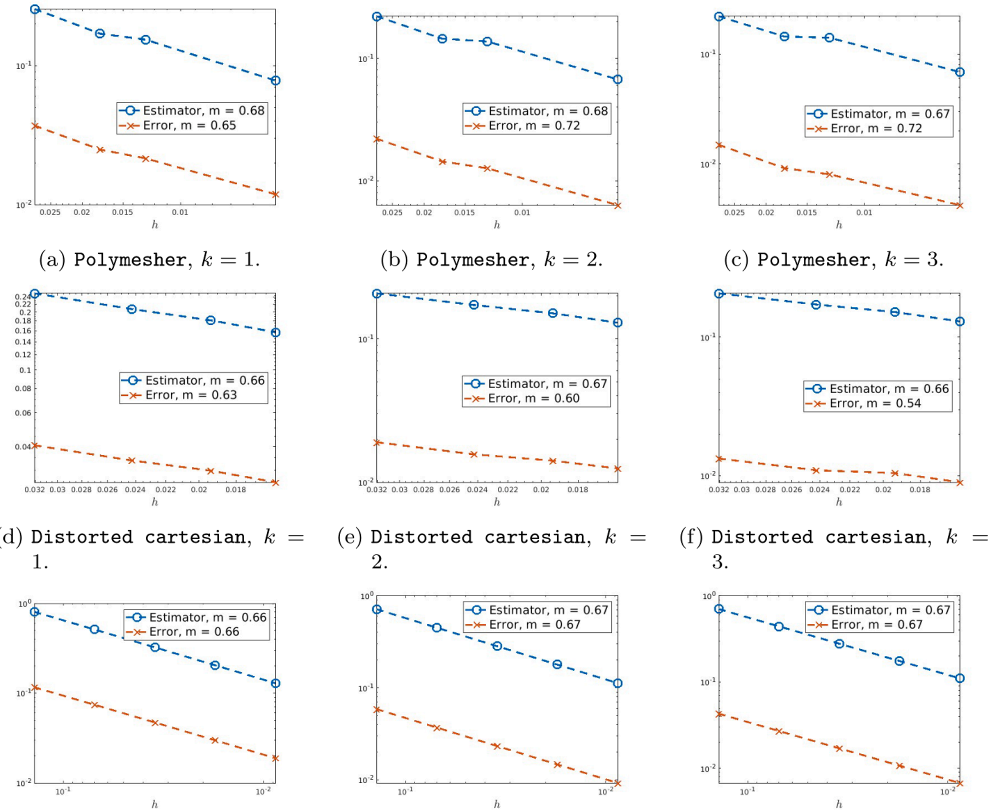

(a) `Polymesher`, $k = 1$. (b) `Polymesher`, $k = 2$. (c) `Polymesher`, $k = 3$.

(d) `Distorted cartesian`, $k = 1$. (e) `Distorted cartesian`, $k = 2$. (f) `Distorted cartesian`, $k = 3$.

(g) `Star concave`, $k = 1$. (h) `Star concave`, $k = 2$. (i) `Star concave`, $k = 3$.

Fig. 6. Test 4: Convergence plots. In the legends, *m* is the average convergence rate.

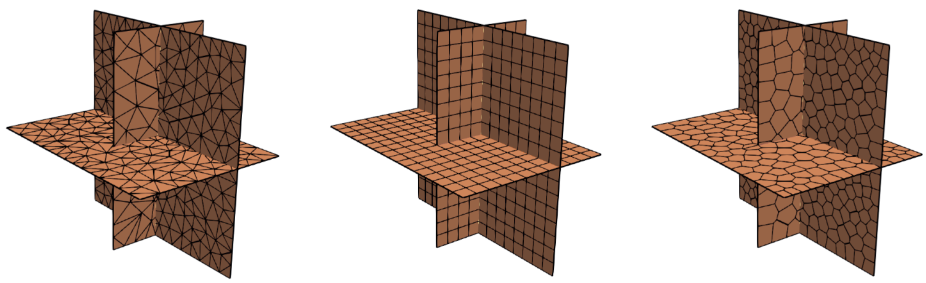

(a) `Triangular` (b) `Squared` (c) `Polygonal`

Fig. 7. Geometry of the DFN considered.

5.5. Test DFN: a discrete fracture network

To validate the robustness of the a posteriori error estimator, we test it on a more practical scenario: a discrete fracture network (DFN), which is a set of planar polygons intersecting in $\mathbb{R}^3$ that models a fractured medium. Flow in DFN is governed by local Darcy laws with matching conditions at intersections, prescribing the continuity of the solution and balance of fluxes [28]. We consider the benchmark problem discussed for instance in [20] , where the DFN is constituted by three fractures as shown in Fig. 7. Exploiting the flexibility of VEM in dealing with aligned edges, we discretize the problem by meshing each fracture independently, and imposing global conformity, as described in [20]. We solve the problem with $\mathcal{K} = I$ on each fracture, by imposing the Dirichlet boundary conditions and the loading term in such a way that the exact solutions are:

$$
\begin{aligned}
u_1(x,y) &= -\frac{1}{10}\left(x+\frac{1}{2}\right)\left(8xy(x^2+y^2)+\operatorname{atan2}(y,x)+x^3\right),\\
u_2(x,z) &= -\frac{1}{10}\left(x+\frac{1}{2}\right)x^3(1-8\pi|z|),\\
u_3(y,z) &= y(y-1)(y+1)(z-1)z,
\end{aligned}
$$

on each corresponding fracture

$$
\begin{aligned}
F_1 &= \left\{(x,y,z)\in\mathbb{R}^3 \,:\, -1\le x\le \frac{1}{2},\ -1\le y\le 1,\ z=0\right\},\\
F_2 &= \left\{(x,y,z)\in\mathbb{R}^3 \,:\, -1\le x\le 0,\ y=0,\ -1\le z\le 1\right\},\\
F_3 &= \left\{(x,y,z)\in\mathbb{R}^3 \,:\, x=-\frac{1}{2},\ -1\le y\le 1,\ -1\le z\le 1\right\}.
\end{aligned}
$$

Following the a posteriori error analysis in [16, Test 5.5], we modify suitably the a posteriori error estimator as:

$$
\tilde{\eta}_E := \frac{h_E^2}{\mathcal{K}_E}\|r_E\|_{0,E}^2 + \frac{1}{2}\sum_{e\in\mathcal{E}_h^E\cap\mathcal{E}_h^{\mathrm{int}}}\frac{h_e}{\mathcal{K}_{\omega_e}}\|j_e\|_{0,e}^2 + \frac{1}{4}\sum_{e\in\mathcal{E}_h^E\cap\mathcal{E}_h^{\mathrm{tr}}}\frac{h_e}{\mathcal{K}_{\omega_e}}\left\|[[\mathcal{K}\,\Pi_{\mathcal{P}}^0\nabla u_{h,i_e}]]_e + [[\mathcal{K}\,\Pi_{\mathcal{P}}^0\nabla u_{h,j_e}]]_e\right\|_{0,e}^2,
$$

where $\Pi_{\mathcal{P}}^0\nabla u_{h,i_e}$ and $\Pi_{\mathcal{P}}^0\nabla u_{h,j_e}$ are the projections of the solutions on the two fractures meeting at an edge e. Moreover, $\mathcal{E}_h^{\mathrm{tr}}$ denotes the set of edges belonging to an intersection and $\mathcal{E}_h^{\mathrm{int}}$ the set of the remaining internal edges. In Fig. 8, we show the computed convergence

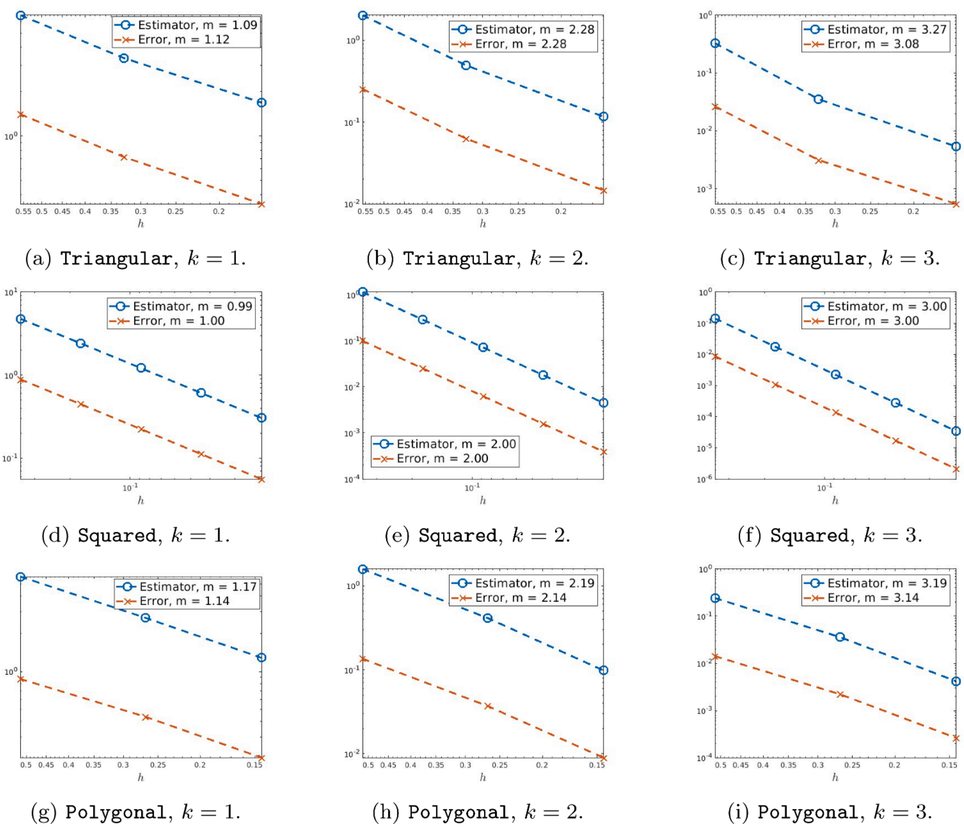

Fig. 8. Test DFN: Convergence plots. In the legends, m is the average convergence rate.

rates on the three meshes, generated by using [29] and depicted in Fig. 7, for the cases $k = 1, 2, 3$. Also in this case, we observe optimal convergence rates and that the effectivity indices are independent of the meshsize.

6. Conclusions

We derived *a posteriori* error estimates for the Stabilization-Free Virtual Element Method defined in [5,6]. The absence of a stabilizing bilinear form in the discretization method allows to obtain equivalence between a suitably defined error measure and classical residual error estimators. Numerical tests on several mesh types validate the proposed error estimator. Finally, we also validate the estimates on a problem of interest in engineering, considering the DFN framework. Results show the robustness of the proposed method in the computation of the pressure distribution.

CRediT authorship contribution statement

Stefano Berrone: Writing – review & editing, Writing – original draft, Validation, Supervision, Software, Resources, Methodology, Investigation, Funding acquisition, Formal analysis, Conceptualization; **Andrea Borio:** Writing – review & editing, Writing – original draft, Validation, Supervision, Software, Resources, Methodology, Investigation, Formal analysis, Conceptualization; **Davide Fassino:** Writing – review & editing, Writing – original draft, Validation, Software, Methodology, Investigation, Formal analysis, Conceptualization; **Francesca Marcon:** Writing – review & editing, Writing – original draft, Validation, Software, Methodology, Investigation, Formal analysis, Conceptualization.

Data availability

Data will be made available on request.

Declaration of competing interest

The authors declare that they have no known competing financial interests or personal relationships that could have appeared to influence the work reported in this paper.

Acknowledgments

The four authors are members of the Gruppo Nazionale Calcolo Scientifico (GNCS) at Istituto Nazionale di Alta Matematica (INdAM). The authors kindly acknowledge financial support by INdAM-GNCS Project 2025 (CUP: E53C24001950001), by the Italian Ministry of University and Research (MUR) through the project MUR-M4C2-1.1-PRIN 2022 (CUP: E53D23005820006), and by the European Union through Next Generation EU, M4C2, PRIN 2022 PNRR project (CUP: E53D23017950001), PNRR M4C2 project of CN00000013 National Centre for HPC, Big Data and Quantum Computing (HPC) (CUP: E13C22000990001) and PRIN project 20227K44ME "Full and Reduced order modelling of coupled systems: focus on non-matching methods and automatic learning (FaReX)" (CUP:E53D23005510006).

References

[1] L. Beirão da Veiga, F. Brezzi, A. Cangiani, G. Manzini, L.D. Marini, A. Russo, Basic principles of virtual element methods, Math. Models Methods Appl. Sci. 23 (01) (2013) 199–214. https://doi.org/10.1142/S0218202512500492

[2] L. Beirão da Veiga, F. Brezzi, L.D. Marini, A. Russo, The Hitchhiker's guide to the virtual element method, Math. Models Methods Appl. Sci. 24 (08) (2014) 1541–1573. https://doi.org/10.1142/S021820251440003X

[3] A.M. D'Altri, S. de Miranda, L. Patruno, E. Sacco, An enhanced VEM formulation for plane elasticity, Comput Methods Appl. Mech. Eng. 376 (2021) 113663. https://doi.org/10.1016/j.cma.2020.113663

[4] S. Berrone, A. Borio, F. Marcon, Lowest order stabilization free virtual element method for the 2D poisson equation, Comput. Math. Appl. 177 (2025) 78–99. https://doi.org/10.1016/j.camwa.2024.11.017

[5] S. Berrone, A. Borio, F. Marcon, A stabilization-free virtual element method based on divergence-free projections, Comput. Methods Appl. Mech. Eng. 424 (2024) 116885. https://doi.org/10.1016/j.cma.2024.116885

[6] S. Berrone, A. Borio, D. Fassino, F. Marcon, Stabilization-free virtual element method for 2D second order elliptic equations, Comput. Methods Appl. Mech. Eng. 438 (2025) 117839. https://doi.org/10.1016/j.cma.2025.117839

[7] A. Borio, C. Lovadina, F. Marcon, M. Visinoni, A lowest order stabilization-free mixed virtual element method, Comput. Math. Appl. 160 (2024) 161–170. https://doi.org/10.1016/j.camwa.2024.02.024

[8] F. Marcon, D. Mora, A stabilization-free virtual element method for the convection-diffusion eigenproblem, J. Sci. Comput. 102 (2) (2025). https://doi.org/10.1007/s10915-024-02765-1

[9] B. Xu, Y. Wang, P. Wriggers, Stabilization-free virtual element method for 2D elastoplastic problems, Int. J. Numer. Methods Eng. (2024) e7490. https://doi.org/10.1002/nme.7490

[10] B. Xu, Y. Wang, P. Wriggers, Stabilization-free virtual element method for finite strain applications, Comput. Methods Appl. Mech. Eng. 417 (2023) 116555. https://doi.org/10.1016/j.cma.2023.116555

[11] A. Chen, N. Sukumar, Stabilization-free virtual element method for plane elasticity, Comput. Math. Appl. 138 (2023) 88–105. https://doi.org/10.1016/j.camwa.2023.03.002

[12] A. Chen, N. Sukumar, Stabilization-free serendipity virtual element method for plane elasticity, Comput. Methods Appl. Mech. Eng. 404 (2023) 115784. https://doi.org/10.1016/j.cma.2022.115784

[13] B. Xu, P. Wriggers, 3D stabilization-free virtual element method for linear elastic analysis, Comput. Methods Appl. Mech. Eng. 421 (2024) 116826. https://doi.org/10.1016/j.cma.2024.116826

[14] A. Lamperti, M. Cremonesi, U. Perego, C. Lovadina, A. Russo, A Hu-Washizu variational approach to self-stabilized virtual elements: 2D linear elastostatics, Comput. Mech. 71 (2023) 935-955. https://doi.org/10.1007/s00466-023-02282-2

[15] F.S. Liguori, A. Madeo, S. Marfia, G. Garcea, E. Sacco, A stabilization-free hybrid virtual element formulation for the accurate analysis of 2D elasto-plastic problems, Comput. Methods Appl. Mech. Eng. 431 (2024) 117281. https://doi.org/10.1016/j.cma.2024.117281

[16] S. Berrone, A. Borio, A residual a posteriori error estimate for the virtual element method, Math. Models Methods Appl. Sci. 27 (8) (2017) 1423–1458. https://doi.org/10.1142/S0218202517500233

[17] A. Cangiani, E.H. Georgoulis, T. Pryer, O.J. Sutton, A posteriori error estimates for the virtual element method, Numerische Mathematik 137 (4) (2017) 857–893. https://doi.org/10.1007/s00211-017-0891-9

[18] P.F. Antonietti, S. Berrone, A. Borio, A. D'Auria, M. Verani, S. Weisser, Anisotropic a posteriori error estimate for the virtual element method, IMA J. Numer. Anal. (2021). https://doi.org/10.1093/imanum/drab001

[19] M. Munar, A. Cangiani, I. Velásquez, Residual-based a posteriori error estimation for mixed virtual element methods, Comput. Math. Appl. 166 (2024) 182–197. https://doi.org/10.1016/j.camwa.2024.05.011

[20] S. Berrone, F. Vicini, Effective polygonal mesh generation and refinement for VEM, Math. Comput. Simul. 231 (2025) 239–258. https://doi.org/10.1016/j.matcom.2024.12.007

[21] L. Beirão da Veiga, C. Canuto, R.H. Nochetto, G. Vacca, M. Verani, Adaptive VEM: stabilization-free a posteriori error analysis and contraction property, SIAM J. Numer. Anal. 61 (2) (2023) 457–494. https://doi.org/10.1137/21M1458740

[22] C. Canuto, D. Fassino, Higher-order adaptive virtual element methods with contraction properties, Math. Eng. 5 (6) (2023) 1–33. https://doi.org/10.3934/mine.2023101

[23] S. Berrone, D. Fassino, F. Vicini, 3D Adaptive VEM with stabilization-free a posteriori error bounds, J. Sci. Comput. 103 (35) (2025). https://doi.org/10.1007/s10915-025-02852-x

[24] M. Petzoldt, A posteriori error estimators for elliptic equations with discontinuous coefficients, Adv. Comput. Math. 16 (1) (2002) 47–75.

[25] S. Berrone, Robust a posteriori error estimates for finite element discretizations of the heat equation with discontinuous coefficients, ESAIM: Modélisation mathématique et analyse numérique 40 (6) (2006) 991–1021. https://doi.org/10.1051/m2an:2006034

[26] R. Verfürth, A review of a posteriori error estimation and adaptive mesh-refinement techniques, Wiley-Teubner, 1996.

[27] C. Talischi, G.H. Paulino, A. Pereira, I.F.M. Menezes, PolyMesher: a general-purpose mesh generator for polygonal elements written in matlab, Struct. Multidiscipl. Optim. 45 (3) (2012) 309–328. https://doi.org/10.1007/s00158-011-0706-z

[28] P.M. Adler, J.-F. Thovert, Fractures and Fracture Networks, 15 of *Theory and Applications of Transport in Porous Media*, Springer Netherlands, Dordrecht, Dordrecht, 1999. https://doi.org/10.1007/978-94-017-1599-7

[29] S. Berrone, A. Borio, G. Teora, F. Vicini, POLYDIM: A C++ library for POLYtopal DIscretization methods, Comput. Phys. Commun. 320 (2026) 109937. https://doi.org/10.1016/j.cpc.2025.109937